The Identification of 1,6′- and 1,3″-Di-*N*-(L-4-amino-2-hydroxybutyryl) Derivatives of Kanamycin as Synthetic Byproducts of Amikacin

GEEWANANDA GUNAWARDANA*,†, CURTIS CHILDRESS†, MERIDITH TRIPP†, XIAOLIN ZHANG†† and PAUL WEST††

†Hospital Products Division, ††Pharmaceutical Products Division, Abbott Laboratories, Abbott Park, IL Chicago, IL 60064-3500, U.S.A.

(Received for publication June 2, 1997)

The investigation of the impurity profile of amikacin (**1**) bulk drug led to the identification of two new derivatives of kanamycin (**2**): 1,6′-di-*N*-(L-4-amino-2-hydroxybutyryl)kanamycin (**3**) and 1,3″-di-*N*-(L-4-amino-2-hydroxybutyryl)kanamycin (**4**).

Amikacin (**1**), a semisynthetic antibiotic derived from acylation of the C-1 amino group of the 2-deoxystreptamine (DOS) moiety of **2** with L(−)-4-amino-2-hydroxybutyric acid (HABA) (**5**), was developed to overcome the emerging resistance of bacteria to aminoglycoside antibiotics and is used in the treatment of infections caused by Gram-negative bacilli. Its synthesis, structure, and the three possible regeoisomers (**6**～**8**) were described by KAWAGUCHI.[1,2] The method described in the U.S. Pharmacopeal Forum (PF) for the assay of amikacin and amikacin sulfate injection refers to a diacyl derivative, labeled as diHABA kanamycin, as an impurity but it does not identify the acylation pattern of this compound.[3] During our investigation of the impurities of amikacin bulk drug, two new compounds were encountered and their structure elucidation was carried out using 2D NMR experiments.[4~6]

Results and Discussion

The two compounds, **3** and **4**, isolated as byproducts of the **1** synthesis, gave HPLC peaks at 19.7 and 15.9 minutes, respectively, when chromatographed according to the PF method. The amikacin peak elutes at 19 minutes, while the peaks for isomers **6**～**8** elute later than 23 minutes in this method. This method involves the derivatization of the analytes with 2,4,6-trinitrobenzenesulfonic acid, followed by separation on a C18 column using phosphate buffer and methanol and detection at 340 nm. Both compounds produced molecular ions at *m/z* 687 $[M+H]^+$ on FAB-MS, indicating that they are both diacyl derivatives of **2**. Compound **3**, a white solid decomposing at 160°C $[\alpha]^{23}$ +3° (*c* 3, H_2O), was found to have the molecular formula $C_{26}H_{51}N_6O_{15}$ (FAB HR-MS observed *m/z* for $C_{26}H_{51}N_6O_{15}$ 687.3401, calc for $C_{26}H_{51}N_6O_{15}$ 687.3412, $\Delta = -1.6$ ppm) and its ^{13}C (DEPT) spectrum revealed the presence of 7 methylene, 17 methine, and 2 quaternary carbons, accounting for all 26 carbons.

The proton signals at 5.16 and 5.6 ppm, which can be assigned, based on their chemical shifts, to the two anomeric protons on the two sugar moieties, 3-amino-3-deoxy-D-glucose (3-AG) and 6-amino-6-deoxy-D-glucose (6-AG), provided good entry points for the analysis of the 2D NMR spectra. The individual proton spin systems for the two moities can be identified and the connectivity between the anomeric protons and the respective methylene protons established using COSY and TOCSY experiments. The signals at 5.16 and 3.79 ppm belong to one spin system, while the signals at 5.6, 3.47, and 3.16 ppm belong to the second spin system. The HMQC experiment showed that the methylene protons resonating at 3.47 and 3.16 ppm are directly attached to the carbon resonating at 43.4 ppm, while the methylene protons resonating at 3.79 ppm are directly attached to the carbon resonating at 63.2 ppm. The two carbon

Fig. 1.

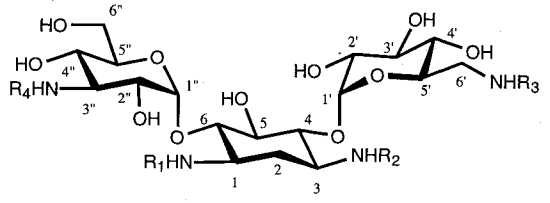

1	R_1=HABA, $R_2=R_3=R_4$=H	Amikacin
2	$R_1=R_2=R_3=R_4$=H	Kanamycin
3	$R_1=R_4$=HABA, $R_2=R_3$=H	1,3″ di-HABA kanamycin
4	$R_1=R_3$=HABA, $R_2=R_4$=H	1,6′ di-HABA kanamycin
6	$R_1=R_3=R_4$=H, R_2=HABA	BB-K29
7	$R_1=R_2=R_3$=H, R_4=HABA	BB-K11
8	$R_1=R_2=R_4$=H, R_3=HABA	BB-K6

HABA=CO·CHOH·CH_2·CH_2·NH_2

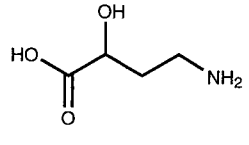

5 L(−)-4-Amino-2-hydroxybutyric acid

* Address for correspondence: D47P, AP9A, 100 Abbot Parkway, Abbott Park, IL 60064-3500, U.S.A.

Table 1. ^1H Chemical shifts (δ, ppm) in D_2O at 500 MHz.

Carbon No.	1	3	4	6	7
1	3.98	4.09	4.09	3.56	3.6
2	1.96, 1.43	2.23, 1.87	2.25, 1.85	2.21, 1.95	2.56, 2.03
3	2.95	3.57	3.50	4.12	3.62
4	3.35	3.94	3.83	3.83	4.01
5	3.75	3.93	3.86	3.86	3.96
6	3.74	3.86	3.86	3.81	3.81
1′	5.34	5.6	5.43	5.58	5.64
2′	3.61	3.69	3.63	3.55	3.67
3′	3.72	3.81	3.76	3.57	3.81
4′	3.33	3.38	3.32	3.36	3.37
5′	3.80	4.04	3.88	3.80	4.01
6′	3.00, 2.80	3.47, 3.16	3.61	3.42, 3.20	3.47, 3.17
1″	5.08	5.16	5.18	5.15	5.14
2″	3.39	3.67	3.81	3.97	3.83
3″	2.99	4.11	3.41	3.52	4.17
4″	3.32	3.56	3.71	3.73	3.58
5″	4.00	4.09	4.09	3.93	3.96
6″	3.78	3.79	3.81	3.81	3.81, 3.77
α	4.19	4.38	4.35, 4.29	4.35	4.39
β	1.92, 1.77	2.18, 2.04	2.18, 1.99	2.23, 2.03	2.19, 2.03
γ	2.79	3.16	3.17	3.18	3.17

Table 2. ^{13}C Chemical shift (δ, ppm) recorded in D_2O at 125 MHz.

Carbon No.	1	3	4	6	7
1	52.4	51.7	51.6	53.3	52.9
2	37.0	33.0	33.1	32.7	30.4
3	51.4	51.0	51.6	50.2	50.8
4	89.5	81.5	83.4	80.7	80.5
5	77.4	75.8	76.2	78.0	75.7
6	83.2	82.9	82.5	86.8	86.7
1′	102.3	98.6	101	100.7	98.8
2′	74.7	73.8	74.2	74.2	73.8
3′	75.7	75.1	75.1	75.2	74.9
4′	73.8	74.0	73.4	73.7	74.0
5′	75.7	71.6	74.1	71.1	71.6
6′	44.3	43.4	42.2	43.2	43.5
1″	101.1	101.3	100.8	103.3	103.9
2″	74.4	72.2	70.9	71.1	72.6
3″	56.9	56.7	58.2	57.9	56.7
4″	72.1	70.0	68.4	68.3	69.8
5″	74.8	75.4	74.8	75.6	76.1
6″	63.1	63.2	62.6	62.8	63.4
α	72.7	72.5, 72.6	72.5, 72.3	72.5	72.7
β	38.4	33.7, 33.8	33.9, 33.7	34.1	33.9
γ	40	39.5, 39.9	39.8, 39.5	39.3	39.4
CONH	179.1	179.5, 178.4	178.8, 178.4	178.0	179.7

signals were assigned to C-6′ ($-CH_2NH_2$) and C-6″ ($-CH_2OH-$) respectively, based on chemical shift information. This allowed the proton signals at 5.6 and 5.16 ppm to be assigned to H-1′ and H-1″, respectively.

The H-1″ signal also showed long-range correlations to carbon signals at 75.4, 72.2, and 56.7 ppm which are directly attached to protons resonating at 4.09, 3.67, and 4.11 ppm, respectively. Based on its chemical shift, the signal at 56.7 ppm can be assigned to C-3″. The H-6″ signal at 3.79 ppm showed long-range correlation to the signal at 75.4 ppm, allowing the assignment of the this signal to C-5″ and the signal at 72.2 to C-2″. The remaining signal at 70.0 ppm thus can be assigned to C-4″. The long-range correlation between the H-3″ signal and the carbonyl carbon signal at 179.5 ppm confirmed that the 3″ amino function of 3-AG is acylated. Further, the anomeric proton signal at 5.16 (H-1″) ppm showed long-range coupling to a carbon signal at 82.9 ppm, allowing the assignment of the latter to C-6 on the DOS moiety.

The signal at 3.16 ppm, due to one of the 6′ protons, showed long-range correlations to the carbon signals at 74.0 and 71.6 ppm. They can be assigned to carbons C-4′ and C-5′, respectively as only the latter showed a long-range correlation with the H-1′ signal. The H-1′ signal also showed long-range correlations to signals at 75.1 and 73.8 ppm, which were directly attached to protons resonating at 3.81 and 3.69 ppm, respectively. However, only the proton signal at 3.69 ppm showed coupling to the H-1′ signal in the DQCOSY spectrum allowing the assignment of signals at 75.1 and 73.8 to C-3′ and C-2′, respectively. Further, the long-range correlation between the H-1′ signal and the carbon signal at 81.5 ppm allowed the latter signal to be assigned to C-4 on the DOS moiety.

The ^{13}C signals for C-4 and C-6 on the DOS moiety were established earlier. The only methylene carbon signal in the system at 33.1 ppm can be assigned to C-2, while the low-field methine carbon signal at 75.8 ppm can be assigned to C-5 based on its chemical shift, leaving the assignment of the methine carbon signals at 51.0 and 51.7 ppm. The H-4 signal at 3.94 ppm showed a long-range correlation to the signal at 51.0 ppm, allowing it to be assigned to C-3 while the H-6 signal at 3.86 showed correlation to the signal at 51.7 ppm, allowing its assignment to C-1. Correlations from H-1 to C-6 and H-3 to C-4 were also observed further confirming this assignment. The H-1 signal at 4.09 ppm showed a long-range correlation to the carbonyl carbon signal at 178.4 ppm, indicating the position of the acylation at C-1 on

the DOS moiety, as expected from the synthetic pathway. Therefore, compound **3** was identified as 1,3″-di-*N*-(L-4-amino-2-hydroxybutyryl)kanamycin.

Similar analysis of the 2D NMR data allowed the unambiguous assignment of all ^{1}H and ^{13}C signals for **4** (white solid, Decomp 120°C, $[\alpha]^{23}$ +4° (*c* 3, H_2O), FAB HR-MS observed *m/z* for $C_{26}H_{51}N_6O_{15}$ 687.3401, calc for $C_{26}H_{51}N_6O_{15}$ 687.3412, $\Delta = -2.1$ ppm). The examination of the HMBC spectra of **3** and **4** indicated that, while both compounds are acylated at C-1, they differ in the position of the second acylation. A strong correlation could be observed between the signals for the methylene function on the 6-AG moiety, H-6′, and the carbonyl carbon on the HABA unit, indicating that in **3** the amine function at C-6′ is acylated. Therefore, compound **4** was identified as 1,6′-di-*N*-(L-4-amino-2-hydroxybutyryl)kanamycin. The unambiguous assignments of ^{1}H and ^{13}C spectral data for **3** and **4** are shown in Tables 1 and 2 along with those of **1** and two other **1** related compounds, BB-K29 (**6**) and BB-K11 (**7**). The examination of these data shows that the chemical-shift information alone is of limited utility in assigning the structure for **1** derivatives. The initial structure assignment of **1** and its isomers was based on chemical degradation studies.[1] When limited material does not permit chemical studies, long-range ^{1}H-^{13}C coupling information can be effectively used for the determination of the acylation pattern of **2** derivatives as shown in this investigation. To the best of our knowledge, this is the first report of the two compounds, **3** and **4**.

The amide proton signals, which would have provided crucial structural information, could not be observed for all compounds in partially deuterated solvents under experimental conditions. Tandom mass spectroscopy was also used as a tool for the identification of **1** derivatives. Mass spectra of the product (fragment) ions resulting from the collisionally activated dissociation (CAD) of the $[M+H]^+$ precursor ion were obtained on a JEOL SX102A mass spectrometer at 10 kV acceleration voltage using B/E linked scanning with helium as the collision gas. The major fragmentation pattern for both **3** and **4** included glycosidic and amide bond cleavages. Fragment ions were observed for the DOS and the two AG moieties and their corresponding acylated fragments. The 6′ acylation is characterized by the presence of a peak at *m/z* 174 resulting from the cross-ring fragmentation. Of particular significance is the peak at *m/z* 425 in the MS/MS spectra of both compounds. This peak corresponds to the presence of one HABA derivative on the DOS and the other on the 6-AG or the 3-AG moieties, *i.e.*, 1-6′, 3-6′, 1-3″, and 3-3″ diHABA derivatives. But this fregment would not be present if both HABA derivatives were on the DOS moiety (1-3 di-HABA) or on the AG moieties (6′-3″ diHABA). As no reference sample of the diHABA compound described in the PF monograph could be obtained, no direct comparison could be made with these compounds.

Acknowledgment

All samples of amikacin-related compounds for this study were kindly supplied by Dr. LEONARDO AMBROSINI, Technical Director, ACS Dobfar S. P. A., Trubiano, Italy.

References

1) KAWAGUCHI, H.; T. NAITO, S. NAKAGAWA & K. FUJISAWA: BB-K8, A new semisynthetic aminoglycoside antibiotic. J. Antibiotics 25: 695～708, 1972
2) NAITO, T.; S. NAKAGAWA, Y. ABE, S. TODA, K. FUJISAWA, T. MIYAKI, H. KOSHIYAMA, H. OHKUMA & H. KAWAGUCHI: Aminoglycoside antibiotics. II. Configurational and positional isomers of BB-K8. J. Antibiotics 26: 297～301, 1973
3) Pharmacopeial Forum, The United States Pharmcopeial Convention, Inc., Vol. 21, No. 4, page 939, 1995
4) PIANTINI, V.; O. W. SØRENSON & R. R. ERNEST: Multiple quantum filters for elucidating NMR coupling networks. J. Am. Chem. Soc. 104: 6800～6801, 1982
5) BAX, A. J. & M. F. SUMMERS: H-1 and C-13 assignments from sensitivity-enhanced detection of heteronuclear multiple-bond connectivity by 2D multiple quantum NMR. J. Am. Chem. Soc. 108: 2039～2094, 1986
6) MULLER, L.: Sensitivity enhanced detection of weak nuclei using heteronuclear multiple quantum coherence. J. Am. Chem. Soc. 101: 4481～4484, 1979